Ultrasound-driven viscous streaming, modelled via momentum injection

J. Packer*, D. Attinger** and Y. Ventikos*

* Fluidics and Biocomplexity Group, Department of Engineering Science, University of Oxford
Oxford, OX1 3PJ, U.K. Tel: +44(0)1865-283452, Email: yiannis.ventikos@eng.ox.ac.uk
** Laboratory for Microscale Transport Phenomena, Department of Mechanical Engineering
Columbia University, New York, NY 10027, USA. Email: da2203@columbia.edu

ABSTRACT

Microfluidic devices can use steady streaming caused by the ultrasonic oscillation of one or many gas bubbles in the liquid to drive small scale flow. Such streaming flows are difficult to evaluate, as analytic solutions are not available for any but the simplest cases, and direct computational fluid dynamics models are unsatisfactory due to the large difference in flow velocity between the steady streaming and the leading order oscillatory motion. We develop a multiscale numerical technique which uses two computational fluid dynamics models to find the streaming flow as a steady problem, and validate this model against experimental results performed by Tho *et. al.* [1].

Keywords: acoustic streaming, CFD, lab-on-a-chip, microfluidic devices, multiscale

1 INTRODUCTION

In addition to the first order oscillating flow generated by a gas bubble in a fluid excited by ultrasound pressure waves, a steady second order flow is generated [2]. This is difficult to model with standard computational fluid dynamics (CFD) techniques, due to the difference in time scales exhibited by the first order oscillating flow (O(kHz) or higher) and the steady second order flow (O(10Hz)) in the configurations considered. Were the second order flow to be determined by standard transient CFD modelling, many thousands of cycles would need to be calculated to determine the nature of the steady flow with reasonable accuracy, as the magnitude of the steady flow is many orders lower than that of the first order oscillating flow.

In this paper, a novel technique for modelling this steady flow is proposed, where the second order flow is modelled directly as a steady state problem, and the forcing for the second order flow is calculated from the modelled first order flow.

2 COMPUTATIONAL FLUID DYNAMICS MODELLING

2.1 First order

The first order model involves a standard CFD approach, where the flow is excited by a moving boundary. In this paper the case of a hemispherical bubble in water is considered, where the bubble wall is displaced sinusoidally, modelling periodic volumetric oscillation. The first order simulation is transient, with three full periods of oscillation modelled. This allows post-transient conditions to be reached, confirmed by comparing the results of the second and third period.

2.2 Second order

The second order CFD model predicts the steady streaming expected for the configuration chosen. The model used is the same as that for the first order, but is a steady model. The moving bubble wall is not modelled, and replaced in the simulation with a static boundary at the mean position. To excite the steady streaming flow, forcing terms are calculated from the first order flow, and added to the fluid volume, as momentum sources, in the region where a viscous sub-layer would exist. The method of calculation of the forcing and the layer thickness is outlined below.

3 CALCULATION OF FORCING

3.1 Theory

The momentum injection is calculated following the analysis of Lighthill [3], finding the forcing from the gradients of the Reynolds stresses. If u, v and w are the flow velocities in the three Cartesian directions and $F_{u,v,w}$ is the force per unit volume in each of these directions and ρ the fluid density, the driving force for the steady streaming is:

$$F_u = -\rho \left(\frac{\partial \overline{uu}}{\partial x} + \frac{\partial \overline{uv}}{\partial y} + \frac{\partial \overline{uw}}{\partial z} \right) \quad (1)$$

$$F_v = -\rho \left(\frac{\partial \overline{vu}}{\partial x} + \frac{\partial \overline{vv}}{\partial y} + \frac{\partial \overline{vw}}{\partial z} \right) \quad (2)$$

$$F_w = -\rho \left(\frac{\partial \overline{wu}}{\partial x} + \frac{\partial \overline{wv}}{\partial y} + \frac{\partial \overline{ww}}{\partial z} \right) \quad (3)$$

Therefore, the mean values over one complete cycle of uu, uv, uw, vv, vw and ww are found for each cell. The differentials of these mean values must then be found in order to find the forcing. Once the differentials are known, as covered in section 3.2.2, the forcing can be calculated for each cell by adding the three appropriate partial differentials.

This forcing only affects the viscous sub-layer adjacent to the boundary [4], [5], as outside this layer the forcing is absorbed into a hydrostatic pressure field [5]. Different authors give slightly different approximations to the thickness of this layer, with Lee & Wang giving the thickness as $\delta = \left(\frac{2\mu}{\rho\omega}\right)^{\frac{1}{2}}$ [5] and Marmottant *et. al.* as $\delta = \left(\frac{\mu}{\rho\omega}\right)^{\frac{1}{2}}$[4]. Here δ is the thickness, ν the kinematic viscosity, μ the absolute viscosity, ω the excitation frequency and ρ the fluid density. Recalling that both expressions are approximations, the difference is not considered significant. In this paper, Marmottant *et. al.*'s approximation is used.

3.2 Numerical method

3.2.1 Mean values

From the first order model, the flow velocities u, v and w of each cell in the volume around the bubble wall are found at each time-step for one complete period of oscillation, once post-transient conditions have been reached. For each cell, the values of uu, uv, uw, vv, vw and ww are computed and their mean value is estimated for the complete period.

Therefore values of each mean multiple ($\overline{uu}$, $\overline{uv}$, ...) are known at the centre of each cell. These can be treated as scattered data points, but the differentials in the x, y, and z directions are needed.

3.2.2 Numerical differentiation

In order to find the differentials of the mean values at each location, the approach taken is to find the difference in value and difference in position for three surrounding points, and to find the Cartesian partial derivatives from this by solving the set of three equations of the form:

$$\delta V = \delta x \frac{\partial V}{\partial x} + \delta y \frac{\partial V}{\partial y} + \delta z \frac{\partial V}{\partial z} \quad (4)$$

As we know three sets of $(\delta V, \delta x, \delta y, \delta z)$ we can solve at each point for $(\frac{\partial V}{\partial x}, \frac{\partial V}{\partial y}, \frac{\partial V}{\partial z})$. This must be done for each of $V = (\overline{uu}, \overline{uv}, \ldots)$.

We solve this by solving the equation:

$$\begin{pmatrix} \frac{\partial V}{\partial x} \\ \frac{\partial V}{\partial y} \\ \frac{\partial V}{\partial z} \end{pmatrix} = \begin{pmatrix} \delta x_1 & \delta y_1 & \delta y_1 \\ \delta x_2 & \delta y_2 & \delta y_2 \\ \delta x_3 & \delta y_3 & \delta y_3 \end{pmatrix}^{-1} \begin{pmatrix} \delta V_1 \\ \delta V_2 \\ \delta V_3 \end{pmatrix} \quad (5)$$

where the subscripts 1,2 and 3 refer to the values for the three surrounding points. If the three points chosen are nearly collinear or coplanar, this will lead to an ill-conditioned solution. Consequently the solution is found by selecting the three points in close proximity which give a well-conditioned behaviour. The closest 15 points are found and the best combination of three selected. This is found by considering all possible combinations, and finding a parameter which describes the quality of the solution. First the condition number of the matrix

$$\begin{pmatrix} \delta x_1 & \delta y_1 & \delta y_1 \\ \delta x_2 & \delta y_2 & \delta y_2 \\ \delta x_3 & \delta y_3 & \delta y_3 \end{pmatrix}$$

is found for all possible combinations of points. The higher this condition number, the more poorly conditioned the set of equations is. This is then multiplied by the product of the distances to the three points under consideration. The combination with the lowest value of this parameter is chosen, as it is the well conditioned set of points closest to the point at which the differential is required. This technique was shown always to be sufficient for the calculation of the derivatives.

The differentiation method is essentially a forwards difference method, extended to three dimensions and applied to a scattered data field.

3.2.3 Forcing

Once the differentials of the mean values ($\overline{uu}$, $\overline{uv}$, ...) are known for each cell in the viscous sub-layer region, the forcing can be found from equations 1, 2 and 3. The forcing is then used in the second order steady-state CDF model as a momentum injection to force the steady streaming. The forcing for each cell is used within the *CFD-ACE2007 solver (ESI Group)* package, in which the forcing per unit volume for each forced cell is multiplied by the cell volume to find the absolute force, and this force used in the equilibrium equations used by the solver, allowing the streaming flow to be found.

4 VALIDATION

4.1 Comparison with experimental work by Tho *et. al.*

The numerical modelling technique proposed is tested against the experimental results of Tho *et. al.* [1], as their results give both the streaming generated and the bubble motion for different modes of bubble oscillation.

NSTI-Nanotech 2008, www.nsti.org, ISBN 978-1-4200-8505-1 Vol. 3

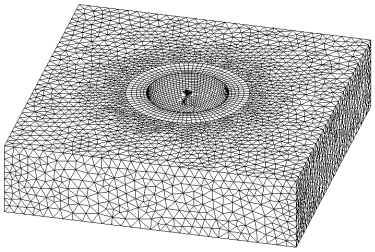

Figure 1: CFD grid

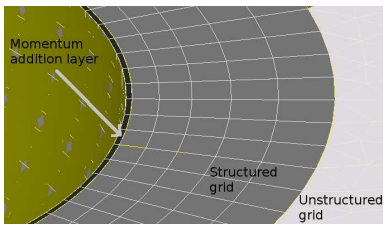

Figure 2: Grid detail

Tho *et. al.*'s experimental conditions correspond to a bubble of mean radius varying between 202 and 274 μm. Several modes of bubble vibration are examined, with case 4 being pure volume oscillation of the bubble. This is the case we chose to present in this paper.

4.1.1 Grid

Tho *et. al.*'s experimental volume is a thin chamber, of height 0.66mm, as described in Figure 1 of Tho *et. al.*'s publication [1]. The hemispherical bubble is on the top wall. Only the region near the bubble is used for our CFD modelling to make the problem more tractable. The grid used is shown in Figure 1. The grid is divided into different volumes so that the required velocities can be output from the first order model, and the forcing applied only to the viscous sub-layer adjacent to the bubble wall in the second order model. These zones are shown in Figure 2.

4.1.2 Boundary conditions

In the first order model, the hemispherical bubble is of radius 270 μm, and the bubble wall is oscillated at 8.658kHz, with a magnitude of 1.41% of the bubble radius, corresponding to case 4 in Tho *et. al.*'s experiments [1]. The boundary condition at the bubble wall is taken as zero slip, since the particles used in the flow visualisation congregate at the interface and allow little slip flow[1]. For comparison a model is also run for zero shear at the bubble wall, which would be expected for perfectly pure fluid, neglecting the viscosity of the bubble gas. The other boundary conditions are the same for the two cases. If the bubble is on the top surface, the top and bottom surfaces have wall boundary conditions (zero tangential and normal flow velocity) and the four edges have fixed pressure boundary conditions, allowing flow between the volume modelled and the large microchamber used experimentally.

4.1.3 Convergence to post-transient conditions

For the first order model, 90 time steps are used per period, and three complete periods modelled. To ensure that the model has reached post-transient conditions, the results of period 2 and 3 are compared and found to be essentially similar, with an average difference of 0.11% between velocities at equivalent time steps within the period.

4.1.4 Data processing

The flow velocities (u,v,w) are found for the volume adjacent to the bubble (the viscous sub-layer volume) and the cells immediately adjacent to this. From the velocity values for the final period (timesteps 181-270), the forcing in the viscous sub-layer is calculated numerically, following the analysis in the section above. All calculations were undertaken with *Octave 2.9*. Due to the grid deformation in the first order model, the position of the cell centres in the layer vary through the period, so their mean positions are used.

4.1.5 Second order model

The same grid and boundary conditions are used for the second order simulation as for the first order transient run, except that the run is steady-state and the bubble wall is maintained in its mean position. The forcing for each cell is added to the viscous sub-layer volume in the simulation, and is the only forcing applied.

4.1.6 Results and discussion

In Tho *et. al.*'s experimental work, the flow velocities are found by a micro-particle image velocimetry (PIV) technique[1]. Tho *et. al.*'s work measures the flow in three planes parallel to the wall on which the bubble is located, which are referred to as the z_1 plane, through the bubble and 75 μm from the wall, the z_2 plane which is 300 μm from the wall and the z_3 plane which is 525 μm from the wall.

Both the velocities predicted in the numerical model, and observed in Tho *et. al.*'s experiment for the volume oscillation case are shown in Table 1. The velocities are seen to be correct to within one order of magnitude, and the accuracy of the predicted flow velocity is better away from the bubble interface. This may be because the PIV method does not pick up the high velocity flow in the small region immediately adjacent to the bubble, as suggested by Tho *et. al.* in section 4.1[1].

Table 1: Comparison of numerical and experimental results. Velocities in mm/s

	Numerical	Tho *et. al.* observed
z_1 plane	1.1	0.3
z_2 plane	0.4	0.3
z_3 plane	0.5	0.3

The pattern of flow predicted by our model, shown in Figures 3 and 4 for the z_1 and z_2 planes is not identical to that observed by Tho *et. al.* for the volume oscillation mode of the bubble, as shown in his Figure 15 [1], but does show interesting similarity with that observed for other modes of vibration, including his case 1 (translating oscillation along a single axis), shown in his Figure 7[1].

A numerical model was also run simulating free-slip conditions at the bubble wall. This gave velocities of an order of magnitude higher than those observed by Tho *et. al.*, suggesting that the assumption of zero slip at the bubble wall due to particle contamination is valid, and a free-slip model invalid for a particle-bearing fluid.

5 CONCLUSION

The multiscale modelling method described can predict the magnitude of steady streaming flows induced by bubble oscillation to within one order of magnitude. Due to the complex nature of both the pressure field and bubble motion in a real forced oscillation fluid/bubble system, the method cannot capture the detail of the flow pattern that will be generated, but suggests one possible mode of flow. This could be improved by computing a first order model which accurately accounts for both the gas bubble, the fluid and the interaction between them generated by an ultrasonic pressure wave. The numerical calculation of the forcing for the steady flow would remain as set out.

ACKNOWLEDGEMENTS

The authors would like to acknowledge Mr Christopher Fenelly for his contributions to early development work on this methodology, and the ESI Group for allowing the use of *CFD-ACE 2007* in this study.

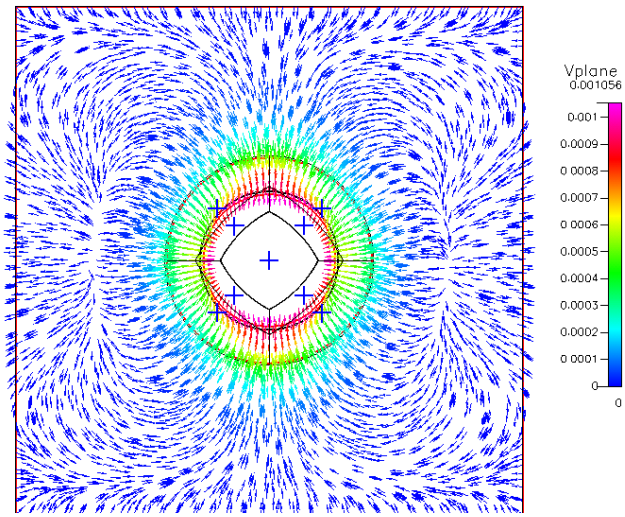

Figure 3: Numerical results, z_1 plane. Velocity in m/s

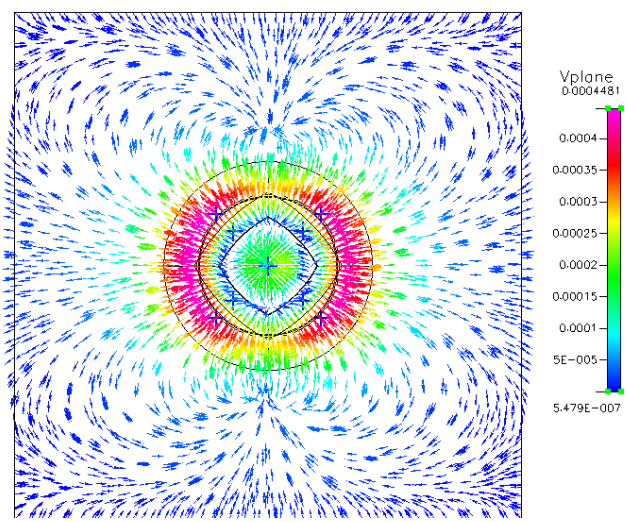

Figure 4: Numerical results, z_2 plane. Velocity in m/s

REFERENCES

[1] Tho, Mannasseh & Ooi, "Cavitation microstreaming patterns in single and multiple bubble systems," J. Fluid Mech., 576, 191-233, 2007.

[2] Xu & Attinger, "Control and ultrasonic actuation of a gas-liquid interface in a microfluidic chip," J. Micromech. Microeng., 17, 609-616, 2007.

[3] Lighthill, "Acoustic Streaming," J. Sound Vib., 63, 391-418, 1978.

[4] Marmottant et. al., "Microfluidics with ultrasound-driven bubbles," J. Fluid Mech., 568, 109-118, 2006.

[5] Lee & Wang, "Outer acoustic streaming," J. Acoust. Soc. Am., 88, 1990.